arXiv:cond-mat/0003511v1 [cond-mat.soft] 31 Mar 2000

Elastic property of single double-stranded DNA molecules: Theoretical study and comparison with experiments

Zhou Haijun[1,2*], Zhang Yang[1], and Ou-Yang Zhong-can[1,3]
[1] *Institute of Theoretical Physics, Academia Sinica, P.O.Box 2735, Beijing 100080, China*
[2] *State Key Lab. of Scientific and Engineering Computing, Beijing 100080, China*
[3] *Center for Advanced Study, Tsinghua University, Beijing 100084, China*
(March 31, 2000, to appear in PRE)

This paper aims at a comprehensive understanding on the novel elastic property of double-stranded DNA (dsDNA) discovered very recently through single-molecule manipulation techniques. A general elastic model for double-stranded biopolymers is proposed and a new structural parameter called the folding angle φ is introduced to characterize their deformations. The mechanical property of long dsDNA molecules is then studied based on this model, where the base-stacking interactions between DNA adjacent nucleotide basepairs, the steric effects of basepairs, and the electrostatic interactions along DNA backbones are taken into account. Quantitative results are obtained by using path integral method, and excellent agreement between theory and the observations reported by five major experimental groups are attained. The strong intensity of the base-stacking interactions ensures the structural stability of DNA, while the short-ranged nature of such interactions makes externally-stimulated large structural fluctuations possible. The entropic elasticity, highly extensibility, and supercoiling property of DNA are all closely related to this account. The present work also suggests the possibility that negative torque can induce structural transitions in highly extended DNA from right-handed B-form to left-handed configurations similar with Z-form configuration. Some formulae concerned with the application of path integral method to polymeric systems are listed in the Appendix.

I. INTRODUCTION

DNA molecule is the primary genetic material of most organisms. It is a double-helical biopolymer in which two chains of complementary nucleotides (the subunits whose sequence constitutes the genetic message) wind (usually right-handedly) around a common axis to form a double-helical structure [1]. Because of this unique structure, the elastic property of DNA molecule influences its biological functions greatly. There are mainly three kinds of deformations in DNA double-helix: stretching and bending of the molecule, twisting of one nucleotide chain relative to its counterpart. All these deformations have vital biological significance. During DNA replication, hydrogen bonds between the complementary DNA bases should be broken and the two nucleotide chains be separated. This strand-separation process requires cooperative unwinding of the double-helix [2]. In DNA recombination reaction, RecA proteins polymerize along DNA template and the DNA molecule is stretched to 1.5 times its relaxed contour length [3,4]. It is suspected that thermal fluctuations of DNA central axis might be very important for RecA polymerization [5]. Another important example is the process of chromosome condensation during prophase of the cell cycle, where the long (circular) DNA chain wraps tightly onto histone proteins and is severely bent [2]. Further more, in living cells DNA chain is usually closed, i.e., the two ends of the molecule is linked together by covalent bonds and the molecule becomes endless. With this chain-closing process, all those quantities characterizing the topological state of the chain are fixed and can only be changed externally by topoisomerases, which are capable of transiently cutting one or both DNA strands and making one strand pass through the other at the cutting point (in the case of type I topoisomerases [6]) or one segment of DNA pass through another (in the case of type II topoisomerases [7,8]). It is possible that this kind of enzyme-induced topology-changing processes are also closely related to the particular mechanic property of DNA molecule. For example, the frequency of collisions between two distant DNA segments in a circular DNA molecule is influenced by the different knot types and different linking numbers (for a definition of this quantity, see below and Sec. II C). A thorough investigation of the deformation and elasticity of DNA will enable us to gain better understanding on many important biological processes concerned with life and growth.

Detailed study on DNA elasticity now becomes possible with the recent experimental developments, including, e.g., optical tweezer methods, atomic force microscopy, fluorescence microscopy. These techniques make it possible to manipulate directly single polymeric molecules and to record their elastic responses with high precision. Experiments done on double-stranded DNA (dsDNA) have revealed that this molecule has very novel elastic property [9–16]. When

a torsionally relaxed DNA is pulled with a force less than 10 picoNewton (pN), its elastic response can be quantitatively understood by regarding the chain as an inextensible thin string with certain bending rigidity (namely, the wormlike chain model [9,17,18]). However, if the external force is increased up to 65 pN, DNA chain becomes highly extensible. At this force, the molecule transit to an over-stretched configuration termed S-DNA, which is 1.6 times longer than the same molecule in its standard B-form structure [11,12]. Besides external forces, it is also possible to apply torsional constraints to DNA double-helix by external torques. The linking number of DNA, i.e., the total topological turns one DNA strand winds around the other, can be fixed at a value larger (less) than the molecule's relaxed value. In such cases we say the DNA molecule is positively (negatively) supercoiled. It is shown experimentally [13] that when external force is less than a threshold value of about 0.3 pN, the extension of DNA molecule decreases with increasing twisted stress and the elastic response of positively supercoiled DNA is similar to that of negatively supercoiled DNA, indicating the DNA chain might be regarded as achiral. However, if the external force is increased to be larger than this threshold, negatively and positively supercoiled DNA molecules behave quite differently. Under the condition of fixed external force between 0.3 pN and 3 pN, while positive twist stress keeps shrinking the DNA polymer, the extension of negatively supercoiled DNA is insensitive to supercoiling degree [13,14]. In higher force region, it is suggested by some authors that positively supercoiled DNA may transit to a configuration called Pauling-like DNA (P-DNA) with exposed nucleotide bases [15], while negative torque may lead to strand-separation in DNA molecule (denaturation of DNA double-helix [14]). A very recent systematic observation performed by Léger *et al.* [16], on the other hand, suggested another possibility that negative supercoiling may result in left-handed Z-form configuration in DNA.

The above-mentioned complicated elastic property revealed by experiments may be directly related to the versatile roles played by DNA molecule in living organisms. Theoretically, to understand DNA elastic property is of current interest. Concerned with one or another aspect of DNA elasticity, models were proposed and valuable insights were obtained (see, for example, Refs. [17–28]), and now it is widely accepted that the competition between DNA bending and torsional deformations deserves to pay considerable attention in understanding the elastic property of DNA molecules. However, it is still a great challenge to understand systematically and quantitatively all aspects of DNA mechanical property based on the same unified framework. What is the intrinsic reason for DNA molecule's entropic elasticity, highly extensibility as well as its supercoiling property? Is it possible for negative torque to stabilize left-handed DNA configurations? These are just some examples of unsolved questions.

In the present work, we have tried to obtain a comprehensive and quantitative understanding on DNA mechanical property. We have thought that the double-stranded nature of DNA structure should be extremely important to its elastic property, and therefore have constructed a general elastic model in which this characteristic is properly taken into account via the introduction of a new structural parameter, the folding angle φ. The elastic property of long dsDNA molecules was then studied based on this model, where the base-stacking interactions between DNA adjacent nucleotide basepairs, their steric effects, and the electrostatic interactions along DNA backbones were all considered. Quantitative results were obtained by using path integral method, and excellent agreement between theory and the experimental observations of several groups were attained. It was revealed that, on one hand, the strong intensity of the base-stacking interactions ensures the structural stability of DNA molecule; while on the other hand, the short-ranged nature of such interactions makes externally-stimulated large structural fluctuations possible. The entropic elasticity, highly extensibility, and supercoiling property of dsDNA molecule are all closely related to this fact. The present work also revealed the possibility that negative torque can induce structural transitions in highly extended DNA from right-handed B-form configuration to left-handed Z-form-like configurations. Some discussions on this respect were performed and we suggested that a possible direct way to check the validity of this opinion is to measure the values of the critical torques under which such transitions are anticipated to take place by the present calculations.

This paper is organized as follows: In Sec. II we introduce the elastic model for dsDNA biopolymers. At the action of an external force, the elastic response of dsDNA molecules is investigated in Sec. III and compared with experimental observations of Smith *et al.* [9,12] and Cluzel *et al.* [11]. Section IV focuses on supercoiled dsDNA molecules, where the relationship between extension and supercoiling degree is obtained numerically and compared with the experiment of Strick *et al.* [13]. From the calculated folding angle distribution, we infer that negative torque can cause structural transitions in dsDNA molecules from right-handed double-helix to left-handed ones. Section V is reserved for conclusion. Two appendices are also presented: in Appendix A we review some basic ideas on the application of path integral method in polymer physics; and in Appendix B we list the matrix elements of the operators in Eq. (15) and Eq. (23). Some parts of this work have been briefly reported in a previous letter [29].

II. ELASTIC MODEL OF DOUBLE-STRANDED DNA MOLECULE

As already stressed, DNA molecule is a double-stranded biopolymer. Its two complementary sugar-phosphate chains twist around each other to form a right-handed double-helix. Each chain is a linear polynucleotide consisting of the following four bases: two purines (A, G) and two pyrimidines (C, T) [1,2]. The two chains are joined together by hydrogen bonds between pairs of nucleotides A-T and G-C. Hereafter, we refer to the two sugar-phosphate chains as the *backbones* and the hydrogen-bonded pairs of nucleotides as the *basepairs*. In this section we discuss the energetics of such an elastic system (see Fig. 1). First of all, the bending energy of the backbones of such double-stranded polymers will be considered; then we will discuss the interactions between DNA basepairs and energy terms related with external fields.

A. Bending and folding deformations

The backbones can be regarded as two inextensible wormlike chains characterized with a very small bending rigidity $\kappa = k_B T \ell_p$, where k_B is Boltzmann's constant and T the environmental temperature, and $\ell_p \simeq 1.5$ nm is the bending persistence length of single-stranded DNA (ssDNA) chains [12]. The bending energy of each backbone is thus expressed as $\kappa \int_0^L (d\mathbf{t}_i/ds)^2 ds$, where $\mathbf{t}_i(s)$ $(i = 1, 2)$ is the unit tangent vector at arclength s along the i-th backbone [30,31], and L is the total contour length of each backbone. The position vectors of the two backbones are expressed as $\mathbf{r}_i(s) = \int^s \mathbf{t}_i(s')ds'$.

Since there are many relatively rigid basepairs between the two backbones in many cases the lateral distance between the backbones can be regarded to be constant and equal to $2R$.[1] In this subsection we focus on the bending energy of the backbones, therefore, for the moment we regard each basepair as a rigid rod of length $2R$ linking between the two backbones and pointing along direction denoted by a unit vector $\mathbf{b}$ from $\mathbf{r}_1$ to $\mathbf{r}_2$ (Fig. 1). Then, $\mathbf{r}_2(s) - \mathbf{r}_1(s) = 2R\mathbf{b}(s)$. In B-form DNA the basepair plane is perpendicular to DNA axis, therefore, in our model relative sliding of the two backbones is not considered and the basepair rod is thought to be perpendicular to both backbones [31], with $\mathbf{b}(s) \cdot \mathbf{t}_1(s) = \mathbf{b}(s) \cdot \mathbf{t}_2(s) \equiv 0$. The central axis of the double-stranded polymer can be defined as $\mathbf{r}(s) = \mathbf{r}_1(s) + R\mathbf{b}(s)$ $[= \mathbf{r}_2(s) - R\mathbf{b}(s) = (\mathbf{r}_1(s) + \mathbf{r}_2(s))/2]$, and its tangent vector is denoted by $\mathbf{t}$. In consistence with actual DNA structures, the central axial tangent $\mathbf{t}$ is also perpendicular to $\mathbf{b}$, i.e., $\mathbf{b}(s) \cdot \mathbf{t}(s) = 0$. (Notice that, however, $\mathbf{t}(s) \neq d\mathbf{r}/ds$; in this paper, s always refers to the arclength of the *backbones*.)

Since all the tangent vectors $\mathbf{t}_1$, $\mathbf{t}_2$, and $\mathbf{t}$ lie on the same plane perpendicular to $\mathbf{b}$, we can write that

$$\begin{aligned} \mathbf{t}_1(s) &= \mathbf{t}(s)\cos\varphi(s) + \mathbf{n}(s)\sin\varphi(s), \\ \mathbf{t}_2(s) &= \mathbf{t}(s)\cos\varphi(s) - \mathbf{n}(s)\sin\varphi(s), \end{aligned} \tag{1}$$

where $\mathbf{n}$ is also a unit vector and $\mathbf{n} = \mathbf{b} \times \mathbf{t}$, and φ is defined as half the rotational angle from $\mathbf{t}_2$ to $\mathbf{t}_1$, with $\mathbf{b}$ being the rotational axis (Fig. 1). We call φ the *folding angle*, and it can vary in the range $(-\pi/2, \ +\pi/2)$, with $\varphi > 0$ corresponding to right-handed rotations and hence right-handed double-helical configurations and $\varphi < 0$ to left-handed ones. With the help of Eq. (1), we know that

$$\frac{d\mathbf{b}}{ds} = \frac{\mathbf{t}_2 - \mathbf{t}_1}{2R} = -\frac{\sin\varphi}{R}\mathbf{n}, \tag{2}$$

and

$$\frac{d\mathbf{r}}{ds} = \frac{1}{2}(\mathbf{t}_1 + \mathbf{t}_2) = \mathbf{t}\cos\varphi. \tag{3}$$

Equation (3) indicates that $\cos\varphi$ measures the extent to which the backbones are "folded" with respect to the central axis. Based on Eqs. (1-3), the total bending energy of the two backbones can be expressed in the following form:

---

[1] In our present work, we have not taken into account the possible deformations of the nucleotide basepairs. In many cases this may be a reasonable assumption. However, under some extreme conditions such kind of deformations may turn to be important. For example, when DNA double-helix is stretched and at the same time is applied with a large positive torque, the nucleotide basepairs may collapse (see Ref. [15] for a description).

$$
\begin{aligned}
E_b &= \frac{\kappa}{2}\int_0^L (\frac{d\mathbf{t}_1}{ds})^2 ds + \frac{\kappa}{2}\int_0^L (\frac{d\mathbf{t}_2}{ds})^2 ds \\
&= \kappa \int_0^L ds \left[(\frac{d\mathbf{t}}{ds})^2 \cos^2\varphi + \sin^2\varphi (\frac{d\mathbf{n}}{ds})^2 + (\frac{d\varphi}{ds})^2 \right] \\
&= \int_0^L ds \left[\kappa (\frac{d\mathbf{t}}{ds})^2 + \kappa (\frac{d\varphi}{ds})^2 + \frac{\kappa}{R^2}\sin^4\varphi \right]. \qquad (4)
\end{aligned}
$$

The bending energy is thus decomposed into the bending energy of the central axis (the first term of Eq. (4)) plus the *folding energy* of the backbones (the second and third terms of Eq. (4)). The physical meanings of these two energy contributions are very clear, and Eq. (4) is very helpful for our following calculations. In Eq. (4), the bending energy of the central axis is very similar with that of a wormlike chain [18], both of which are related to the square of the changing rate of the axial tangent vectors. But there are two important differences: (a) in the derivative $d\mathbf{t}/ds$ of Eq. (4), the arclength parameter s is measured along the backbone, not along the central axis; (b) in the wormlike chain model the central axis is inextensible, while here the central axis is extensible.

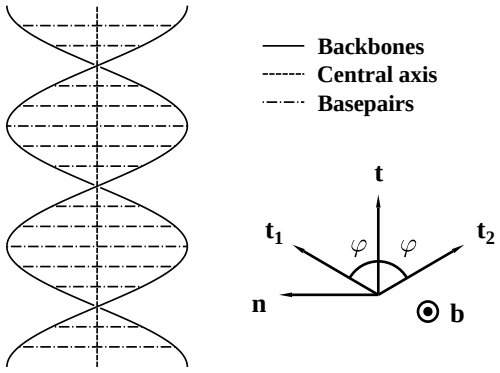

FIG. 1. Schematic representation of a double-stranded DNA model used in this paper. The right part demonstrates the definition of φ on the local $\mathbf{t}-\mathbf{n}$ plane, where $\mathbf{t}$, $\mathbf{t}_1$ and $\mathbf{t}_2$ are, respectively, the tangential vectors of the central axis and the two backbones; φ is the folding angle; and the unit vector $\mathbf{b}=\mathbf{t}\times\mathbf{n}$ is perpendicular to the $\mathbf{t}-\mathbf{n}$ plane.

In deriving Eq. (4), the basepairs are models just as thin rigid rods of fixed length, i.e., the DNA molecule is viewed as a ladder-like structure (see Fig. 1). Actually, however, basepairs form disc-like structures and have finite volume. The steric effects caused by the finite volume of basepairs is anticipated to hinder considerably the bending deformation of the central axis, and hence will increases its bending rigidity greatly [1]. Furthermore, dsDNA molecule is a strong polyelectrolyte, with negatively-charged groups distributed regularly along the chain's surface. The electrostatic repulsion force between these negatively-charged groups will also considerably increase the bending rigidity of the dsDNA chain [1]. To quantitatively take into account the above mentioned two kinds of effects is very difficult. Here we treat this problem phenomenologically by simply replacing the bending rigidity κ in the first term of Eq. (4) with a quantity κ^*. It is required that $\kappa^* > \kappa$, and the precise value of κ^* will then be determined self-consistently by the best fitting with experimental data as shown in Sec. III.

B. Base-stacking interactions between basepairs

In Sec. II A, we have discussed in detail the bending energy of dsDNA polymers, which is caused by bending of the backbones as well as steric effects and electrostatic interactions. In dsDNA molecule there is another kind of important interactions, namely the base-stacking interaction between adjacent nucleotide basepairs [1,2]. The base-stacking interactions originate from the weak van der Waals attraction between the polar groups in adjacent nucleotide basepairs. Such interactions are short-ranged and their total effect is usually described by a potential energy of the Lennard-Jones form (6-12 potential [1]). Base-stacking interactions play significant role in stabilization of DNA double-helix. The main reason why DNA can but RNA can not form long double-helix is as follows [32]: Because of the steric interference caused by the hydroxyl group attached to the $2'$ carbon of RNA riboses, the stacking interaction between adjacent RNA nucleotide basepairs is very weak and can not stabilize the formed double-helical

structure; while in the DNA ribose, it is a hydrogen atom attached to its $2'$ carbon and serious steric interference is avoided (fortunately!).

In a continuum theory of elasticity, the summed total base-stacking potential energy is converted into the form of the following integration:

$$E_{LJ} = \sum_{i=1}^{N-1} U_{i,i+1} = \int_0^L \rho(\varphi) ds, \tag{5}$$

where $U_{i,i+1}$ is the base-stacking potential between the i-th and the $(i+1)$-th basepair, N is the total number of basepairs, and the base-stacking energy density ρ is expressed as

$$\rho(\varphi) = \begin{cases} \frac{\epsilon}{r_0}[(\frac{\cos\varphi_0}{\cos\varphi})^{12} - 2(\frac{\cos\varphi_0}{\cos\varphi})^6] & (\text{for } \varphi \geq 0), \\ \frac{\epsilon}{r_0}[\cos^{12}\varphi_0 - 2\cos^6\varphi_0] & (\text{for } \varphi < 0). \end{cases} \tag{6}$$

In Eq. (6), the parameter r_0 is the *backbone* arclength between adjacent bases ($r_0 = L/N$); φ_0 is a parameter related to the equilibrium distance between a DNA dimer ($r_0 \cos\varphi_0 \sim 3.4$ $\mathring{A}$); and ϵ is the base-stacking intensity which is generally base-sequence specific [1]. In this paper we focus on macroscopic properties of long DNA chains composed of relatively random sequences, therefore we just consider ϵ in the average sense and take it as a constant, with $\epsilon \simeq 14.0\ k_BT$ as averaged over quantum-mechanically calculated results on all the different DNA dimers [1].

The asymmetric base-stacking potential Eq. (6) ensures a relaxed DNA to take on a right-handed double-helix configuration (i.e., the B-form) with its folding angle $\varphi \sim \varphi_0$. To deviate the local configuration of DNA considerably from its B-form generally requires a free energy of the order of ϵ per basepair. Thus, DNA molecule will be very stable under normal physiological conditions and thermal energy can only make it fluctuate very slightly around its equilibrium configuration, since $\epsilon \gg kT$. Nevertheless, although the stacking intensity ϵ in dsDNA is very strong compared with thermal energy, the base-stacking interaction by its nature is short-ranged and hence sensitive to the distance between the adjacent basepairs. If dsDNA chain is stretched by large external forces, which cause the average inter-basepair distance to exceed some threshold value determined intrinsically by the molecule, the restoring force provided by the base-stacking interactions will no longer be able to offset the external forces. Consequently, it will be possible that the B-form configuration of dsDNA will collapse and the chain will turn to be highly extensible. Thus, on one hand, the strong base-stacking interaction ensures the standard B-form configuration to be very stable upon thermal fluctuations and small external forces (this is required for the biological functions of DNA molecule to be properly fulfilled [2]); but on the other hand, its short-rangedness gives it considerable latitude to change its configuration to adapt to possible severe environments (otherwise, the chain may be pulled break by external forces, for example, during DNA segregation [2]). This property of DNA base-stacking interactions is very important to dsDNA molecule. As we will see in Secs. III and IV, the mechanical property of DNA chain is indeed closely related to the above-mentioned insight.

C. External forces and torques

In the previous two subsections, we have described the intrinsic energy of DNA double-helix. Experimentally, to probe the elastic response of linear DNA molecule, the polymer chain is often pulled by external force fields and/or untwisted or overtwisted by external torques. To study the mechanic response of dsDNA molecule, we consider in this subsection the energy terms related to external forces and torques in our theoretical framework.

For the external force fields, here we constrained ourselves to the simplest situation where one terminal of DNA molecule is fixed and the other terminal is pulled with a force $\mathbf{F} = f\mathbf{z}_0$ along direction of unit vector $\mathbf{z}_0$ [9]. (In fact, hydrodynamic fields or electric fields are also frequently used to stretch semiflexible polymers [33], but we will not discuss such cases in this paper.) The end-to-end vector of a DNA chain is expressed as $\int_0^L \mathbf{t}(s)\cos\varphi(s)ds$ according to Eq. (3). Then the total "potential" energy of the chain in the external force field is

$$E_f = -\int_0^L \mathbf{t}\cos\varphi ds \cdot \mathbf{F} = -\int_0^L f\mathbf{t}\cdot\mathbf{z}_0\cos\varphi ds. \tag{7}$$

In the experimental setup, external torques can be applied on linear dsDNA molecule by the following procedure: first, DNA ligases are used to ligate all the possible single-stranded nicks; then the two strands of dsDNA molecule at one end are fixed onto a template, while the two strands at the other end is attached tightly to a magnetic bead; afterwards, torques are introduced into DNA double-helix by rotating the magnet bead with an external magnetic field

[11,15]. Torque energy is then related to the topological turns caused by the external torque on DNA double-helix. The total number of topological turns one DNA strand winds around the other, which is usually termed the total linking number Lk [34–36], is expressed as the sum of the twisting number, $Tw(\mathbf{r}_1(\mathbf{r}_2),\mathbf{r})$ of backbone $\mathbf{r}_1$ (or $\mathbf{r}_2$) around the central axis $\mathbf{r}$ and the writhing number $Wr(\mathbf{r})$ of the central axis; i.e., $Lk = Tw + Wr$. According to Refs. [35–37] and Eq. (2), we obtain that

$$Tw(\mathbf{r}_1,\mathbf{r}) = \frac{1}{2\pi}\int_0^L \mathbf{t}\times\mathbf{b}\cdot\frac{d\mathbf{b}}{ds}ds = \frac{1}{2\pi}\int_0^L \frac{\sin\varphi}{R}ds. \tag{8}$$

The writhing number of the central axis is generally much more difficult to calculate. It is expressed as the following Gauss integral over the central axis [34]:

$$Wr(\mathbf{r}) = \frac{1}{4\pi}\int\int \frac{d\mathbf{r}\times d\mathbf{r}'\cdot(\mathbf{r}-\mathbf{r}')}{|\mathbf{r}-\mathbf{r}'|^3}. \tag{9}$$

In the case of linear chains, provided that some fixed direction (for example the direction of the external force, $\mathbf{z}_0$) can be specified and that the tangent vector $\mathbf{t}$ never points to $-\mathbf{z}_0$ (i.e., $\mathbf{t}\cdot\mathbf{z}_0 \neq -1$), it was proved by Fuller that the writhing number Eq. (9) can be calculated alternatively according to the following formula [38]:

$$Wr(\mathbf{r}) = \frac{1}{2\pi}\int_0^L \frac{\mathbf{z}_0\times\mathbf{t}\cdot d\mathbf{t}/ds}{1+\mathbf{z}_0\cdot\mathbf{t}}ds. \tag{10}$$

The above equation can be further simplified for highly extended linear DNA chains whose tangent $\mathbf{t}$ fluctuates only slightly around $\mathbf{z}_0$. In this case, Eq. (10) leads to the approximate expression that

$$Wr(\mathbf{r}) \simeq \frac{1}{4\pi}\int_0^L \left[-t_y\frac{dt_x}{ds} + t_x\frac{dt_y}{ds}\right]ds, \tag{11}$$

where t_x and t_y are, respectively, the two components of $\mathbf{t}$ with respect to two arbitrarily chosen orthonormal directions ($\mathbf{x}_0$ and $\mathbf{y}_0$) on the plane perpendicular to $\mathbf{z}_0$.

The energy caused by the external torque of magnitude Γ is then equal to

$$E_t = -2\pi\Gamma Lk = -2\pi\Gamma(Tw+Wr). \tag{12}$$

To conclude this section, the total energy of a dsDNA molecule under the action of an external force and an external torque is expressed as

$$\begin{aligned} E &= E_b + E_{LJ} + E_f + E_t \\ &= \int_0^L \left[\kappa^*(\frac{d\mathbf{t}}{ds})^2 + \kappa(\frac{d\varphi}{ds})^2 + \frac{\kappa}{R^2}\sin^4\varphi + \rho(\varphi) - f\mathbf{t}\cdot\mathbf{z}_0\cos\varphi - \frac{\Gamma}{R}\sin\varphi - \Gamma\frac{\mathbf{z}_0\times\mathbf{t}\cdot d\mathbf{t}/ds}{1+\mathbf{z}_0\cdot\mathbf{t}}\right]ds \qquad (13) \\ &\simeq \int_0^L \left[\kappa^*(\frac{d\mathbf{t}}{ds})^2 + \kappa(\frac{d\varphi}{ds})^2 + \frac{\kappa}{R^2}\sin^4\varphi + \rho(\varphi) - f\mathbf{t}\cdot\mathbf{z}_0\cos\varphi - \frac{\Gamma}{R}\sin\varphi + \frac{\Gamma}{2}t_y\frac{dt_x}{ds} - \frac{\Gamma}{2}t_x\frac{dt_y}{ds}\right]ds. \qquad (14) \end{aligned}$$

Notice that Eq. (14) can be applied only in the case of highly extended DNA. In the following two sections, we will study the mechanical property of single dsDNA molecules based on the model energy Eq. (13) and Eq. (14). The theoretical results will be compared with experimental observations and discussed.

III. EXTENSIBILITY AND ENTROPIC ELASTICITY OF DNA

In this section we investigate the elastic responses of single DNA molecules under the actions of external forces based on the model introduced in Sec. II. There is no external torque acted, thus $\Gamma = 0$ in Eq. (13). The particular form of the energy function Eq. (13) of the present model makes it convenient for us to study its statistical property by path integral method. In Appendix A a detailed description on the application of path integral method to polymer physics is given [39]. Our calculations in this and the next sections are based on this method.

For a polymer whose energy is expressed in the form of Eq. (13) with $\Gamma = 0$, according to the technique outlined in Appendix A (see Eqs. (A1) and (A7)), the Green equation governing the evolution of the "wave function" $\Psi(\mathbf{t},\varphi;s)$ of the system is obtained to be of the following form:

$$\frac{\partial\Psi(\mathbf{t},\varphi;s)}{\partial s}=\left[\frac{\partial^2}{4\ell_p^*\partial\mathbf{t}^2}+\frac{\partial^2}{4\ell_p\partial\varphi^2}+\frac{f\cos\varphi}{k_BT}\mathbf{t}\cdot\mathbf{z}_0-\frac{\rho(\varphi)}{k_BT}-\frac{\ell_p}{R^2}\sin^4\varphi\right]\Psi(\mathbf{t},\varphi;s), \tag{15}$$

where $\ell_p^*=\kappa^*/k_BT$ and $\ell=\kappa/k_BT$. The spectrum of the above Green equation is discrete and, for a long dsDNA molecule according to Eqs. (A10) and (A13), its average extension can be obtained either by differentiation of the ground-state eigenvalue, g_0, of Eq. (15) with respect to f:

$$\langle Z\rangle=\int_0^L\langle\mathbf{t}\cdot\mathbf{z}_0\cos\varphi\rangle ds=-Lk_BT\frac{\partial g_0}{\partial f}, \tag{16}$$

or by a direct integration with the normalized ground-state eigenfunction, $\Phi_0(\mathbf{t},\varphi)$, of Eq. (15):

$$\langle Z\rangle=L\int|\Phi_0|^2\mathbf{t}\cdot\mathbf{z}_0\cos\varphi d\mathbf{t}d\varphi. \tag{17}$$

Both g_0 an $\Phi_0(\mathbf{t},\varphi)$ can be obtained numerically through standard diagonalization methods and identical results are obtained by Eqs. (16) and (17). Here we just briefly outline the main procedures in converting Eq. (15) into the form of a matrix.

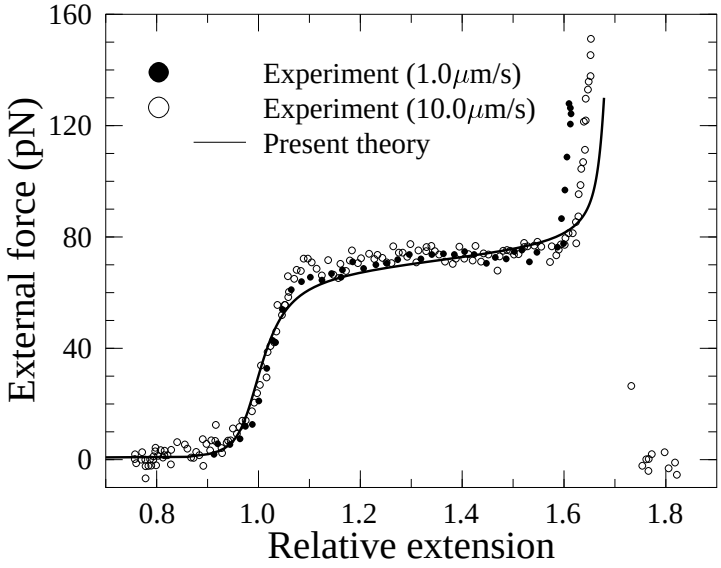

FIG. 2. Force-extension relation of torsionally relaxed DNA molecule. Experimental data is from Fig. 2A of [11](symbols). Theoretical curve is obtained by the following considerations: (a) $\ell_p=1.5$ nm and $\epsilon=14.0k_BT$; (b) $\ell_p^*=53.0/2\langle\cos\varphi\rangle_{f=0}$ nm, $r_0=0.34/\langle\cos\varphi\rangle_{f=0}$ nm and $R=(0.34\times10.5/2\pi)\langle\tan\varphi\rangle_{f=0}$ nm; (c) adjust the value of φ_0 to fit the data. For each φ_0, the value of $\langle\cos\varphi\rangle_{f=0}$ is obtained self-consistently. The present curve is drawn with $\varphi_0=62.0^\circ$ (in close consistence with the structural property of DNA), and $\langle\cos\varphi\rangle_{f=0}$ is determined to be 0.573840. DNA extension is scaled with its **B**-form contour length $L\langle\cos\varphi\rangle_{f=0}$.

Firstly, for our convenience we perform the following transformation:

$$\varphi=\tilde{\varphi}-\frac{\pi}{2}, \tag{18}$$

hence the new argument $\tilde{\varphi}$ can change in the range from 0 to π. Then, we choose the combination of $Y_{lm}(\mathbf{t})$ and $f_n(\tilde{\varphi})$ as the base functions of the Green equation Eq. (15):

$$\Psi(\mathbf{t},\tilde{\varphi};s)=\sum_{lmn}C_{lmn}(s)Y_{lm}(\mathbf{t})f_n(\tilde{\varphi}). \tag{19}$$

In the above expression, $Y_{lm}(\mathbf{t}) = Y_{lm}(\theta, \phi)$ ($l = 0, 1, 2, \cdots; m = 0, \pm 1, \cdots, \pm l$) are the spherical harmonics [40], where θ and ϕ are the two directional angles of $\mathbf{t}$, i.e., $\mathbf{t} = (\sin\theta\cos\phi, \sin\theta\sin\phi, \cos\theta)$; and

$$f_n(\tilde{\varphi}) = \sqrt{\frac{2}{a}} \sin(\frac{n\pi}{a}\tilde{\varphi}) \quad (n = 1, 2, \cdots) \tag{20}$$

are the eigenfunctions of one-dimensional infinitely deep square potential well of width a. [2]

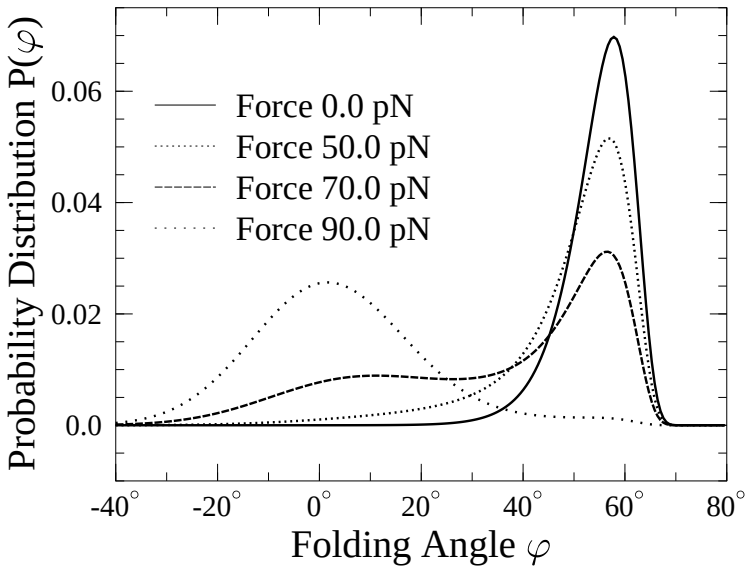

FIG. 3. Folding angle distribution for torsionally relaxed DNA molecules under external forces.

With the wave function Ψ being expanded using the above mentioned base functions, the operator acting on Ψ (i.e., the expression in the square brackets of Eq. (15)) can also be written into matrix form under these base functions. This matrix, whose elements are listed in Appendix B, is then diagolized numerically to obtain its ground-state eigenvalue and eigenfunction. To simplify the calculation, we further notice that in the present case of Eq. (15), the ground-state is independent to ϕ, i.e., m can be set to $m = 0$ in Eq. (19).

The resulting force vs extension relation obtained from Eq. (16) or Eq. (17) is shown in Fig. 2 in the whole relevant force range and compared with the experimental observation of Cluzel *et al.* [11,12]. The theoretical curve in this figure is obtained with just one adjustable parameter (see caption of Fig. 2); the agreement with experiment is excellent. Figure 2 demonstrates that the highly extensibility of DNA molecule under large external forces can be quantitatively explained by the present model.

To further understand the force-induced extensibility of DNA, in Fig. 3 the folding angle distribution of dsDNA molecule is shown, with the external force kept at different values. Here, according to Eq. (A13) the folding angle distribution $P(\varphi)$ is calculated by the following formula:

$$P(\varphi) = \int |\Phi_0(\mathbf{t}, \varphi)|^2 d\mathbf{t}. \tag{21}$$

[2]In the actual calculations, the right boundary of the square well is chosen to be slightly less than π to avoid flush-off of computer memory caused by the divergence of the base-stacking potential Eq. (6) at $\tilde{\varphi} = \pi$. We set $a = 0.95\pi$ in this paper. However, we have checked that the results are almost identical for other values of a, provided that $a \geq 165^\circ$.

Figures 2 and 3, taking together, demonstrate that the elastic behaviors of dsDNA molecule are radically different under the condition of low and large applied forces. In the following, we will discuss them separately.

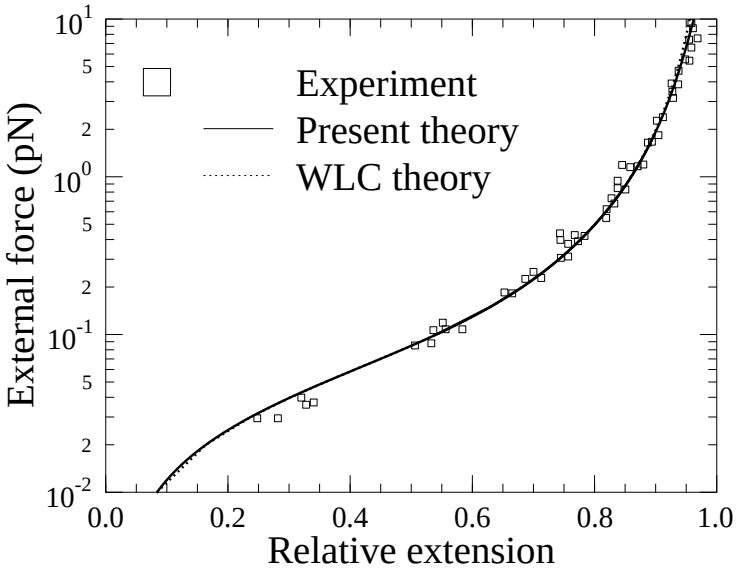

FIG. 4. Low-force elastic behavior of DNA. Here experimental data is from Fig. 5B of [9], the dotted curve is obtained for a wormlike chain with bending persistence length 53.0 nm and the parameters for the slid curve are the same as those in Fig. 2.

The low-force region When external force is low ($\leq$ 10 pN), the folding angle is distributed narrowly around the angle of $\varphi \simeq +57°$, and there is no probability for the folding angle to take on values less than 0° (Fig. 3), indicating that DNA chain is completely in the right-handed B-form configuration with small axial fluctuations. This should be attributed to the strong base-stacking intensity, as pointed out in Sec. II B. Consequently, the elasticity of DNA is solely caused by thermal fluctuations in the axial tangent $\mathbf{t}$ (Fig. 2), and DNA molecule can be regarded as an inextensible chain. This is the physical reason why, in this force region, the elastic behavior of DNA can be well described by the wormlike chain model [17,18,41]. Indeed, as shown in Fig. 4, at forces $\leq$ 10 pN, the wormlike chain model and the present model give identical results. Thus, we can conclude with confidence that, when external fields are not strong, the wormlike chain model is a good approximation of the present model to describe the elastic property of dsDNA molecules; and the bending persistence length of the molecule is $2\ell_p^*\langle\cos\varphi\rangle$, as indicated by Eq. (3) and Eq. (4).

The large-force region With the continuous increase of external pulling forces, the axial fluctuations becomes more and more significant. For example, at forces $\simeq$ 50 pN, although the folding angle distribution is still peaked at $\varphi \simeq 57°$, there is also considerable probability for the folding angle to be distributed in the region $\varphi \sim 0°$ (Fig. 4). Therefore, at this force region, DNA polymer can no longer be regarded as inextensible. At $f \simeq 65$ pN, another peak in the folding angle distribution begins to emerge at $\varphi \simeq 0°$, marking the onset of cooperative transition from B-form DNA to overstretched S-form DNA [11,12]. This is closely related to the short-ranged nature of the base-stacking interactions [1] (see Sec. II B). At even higher forces ($f \geq 80$ pN) [3], the DNA molecule becomes completely into the overstretched form with its folding angle peaked at $\varphi = 0°$.

The force-induced axial fluctuations in DNA double-helix can be biologically significant. For example, it has been demonstrated that axial fluctuations in dsDNA enhance considerably the polymerization of RecA proteins along DNA chain [5,42,43]. An quantitative study on the coupling between RecA polymerization and DNA axial fluctuation is

[3]This threshold f_t of over-stretch force is also consistent with a plain evaluation from base-stacking potential of $\epsilon \sim f_t r_0$, i.e. $f_t \sim 90$ pN.

anticipated to be helpful.

It seems that in the experiments [11,12] the transition to S-DNA occurs even more cooperatively and abruptly than predicted by the present theory (see Fig. 2). This may be related to the existence of single-stranded breaks (nicks) in the dsDNA molecules used in the experiments. Nicks in DNA backbones can lead to strand-separation or relative sliding of backbones [11,12], and they can make the transition process more cooperative. However, the comprehensive agreement achieved in Figs. 2 and 4 indicates that such effects are only of limited significance. The elasticity of DNA is mainly determined by the competition between folding angle fluctuation and tangential fluctuation, which are governed, respectively, by the base-stacking interactions (ϵ) and the axial bending rigidity (κ^*) in Eq. (13).

IV. ELASTIC PROPERTY OF SUPERCOILED DNA

In the preceding section, we have discussed the elastic response of long DNA chains under the action of external forces. In the present section, we turn to study the elasticity of supercoiled DNA double-helix. For this purpose, in the experimental setup, all the possible nicks in the DNA nucleotide strands are ligated [13], and a torque as well as an external pulling force is acting on one terminal of the DNA double-helix, which typically untwists or overtwists the original B-form double-helix to some extent and makes its total linking number (refer to Sec. II C for the definition of the linking number) less or greater than the equilibrium value. We say that such DNA molecules with deficit (excess) linking number are negatively (positively) supercoiled, and define the degree of supercoiling as

$$\sigma = \frac{Lk - Lk_0}{Lk_0}, \tag{22}$$

where Lk_0 represents the linking number of a relaxed DNA of the same contour length. In living organisms, DNA molecules are often negatively supercoiled, with a linking number deficit of about $\sigma = -0.06$. Thus, a detailed investigation on the mechanical property of supercoiled DNA molecules is not only of academic interest but can also help us to understand the possible biological advantages of negative supercoiling.

A. Relationship between extension and supercoiling degree

We focus on the property of highly extended DNA molecules whose tangent vectors fluctuate only slightly around the force direction $\mathbf{z}_0$. According to what we have mentioned in Sec. II C, in this case the approximate energy expression Eq. (14) can be used. The external stretching force is restricted to be greater than 0.3 pN to make sure that the end-to-end distance of DNA chain approaches its contour length (see Fig. 5). Based on Eqs. (14) and (A7), the Green equation for highly stretched and supercoiled dsDNA is then obtained to be

$$\begin{aligned}\frac{\partial \Psi(\mathbf{t},\varphi;s)}{\partial s} = \Bigg[& \frac{\partial^2}{4\ell_p^* \partial \mathbf{t}^2} + \frac{\partial^2}{4\ell_p \partial \varphi^2} + \frac{f\cos\varphi}{k_B T}\mathbf{t}\cdot\mathbf{z}_0 - \frac{\rho(\varphi)}{k_B T} - \frac{\ell_p}{R^2}\sin^4\varphi \\ & + \frac{\Gamma}{R k_B T}\sin\varphi - \frac{\Gamma}{4 k_B T \ell_p^*}\frac{\partial}{\partial\phi} + \frac{\Gamma^2}{16\ell_p^*(k_B T)^2}\sin^2\theta \Bigg] \Psi(\mathbf{t},\varphi;s),\end{aligned} \tag{23}$$

where (θ,ϕ) are the two directional angles of $\mathbf{t}$ as mentioned before in Sec. III. Similar to what we have done in Sec. III, we can now express the above Green equation in matrix form using the combinations of spherical harmonics $Y_{lm}(\theta,\phi)$ and $f_n(\varphi)$ as the base functions. The ground-state eigenvalue and eigenfunction of Eq. (23) can then be obtained numerically for given applied force and torque and the average extension be calculated through Eq. (16) or through the following formula:

$$\langle Z\rangle = L\int \chi_0(\mathbf{t},\varphi)\mathbf{t}\cdot\mathbf{z}_0\cos\varphi\Phi_0(\mathbf{t},\varphi)d\mathbf{t}d\varphi, \tag{24}$$

where $\chi_0(\mathbf{t},\varphi)$ is the ground-state left-eigenfunction of Eq. (23). [4] The writhing number Eq. (11) is calculated according to Eq. (A16) to be

[4] As remarked in Appendix A, because the operator in the square brackets of Eq. (23) acting on $\Psi(\mathbf{t},\varphi;s)$ is not Hermitian, the resulting matrix form of the operator may not be diagonalized by unitary matrices. Consequently, in general $\chi_0(\mathbf{t},\varphi) \neq \Phi_0^*(\mathbf{t},\varphi)$.

$$\langle Wr\rangle = L\frac{\Gamma}{16\pi\ell_p^* k_B T}\int \chi_0(\mathbf{t},\varphi)\sin^2\theta\Phi_0(\mathbf{t},\varphi)d\mathbf{t}d\varphi, \tag{25}$$

and average linking number is then calculated to be

$$\langle Lk\rangle = \langle Tw\rangle + \langle Wr\rangle = \frac{L}{2\pi R}\int \chi_0 \sin\varphi\Phi_0 d\mathbf{t}d\varphi + \frac{L\Gamma}{16\pi\ell_p^* k_B T}\int \chi_0\sin^2\theta\Phi_0 d\mathbf{t}d\varphi. \tag{26}$$

Thus, after we have obtained the ground-state eigenvalue as well as its left- and right-eigenfunction numerically, we can calculate numerically all the quantities of our interest, for example, the average extension, the average supercoiling degree, the folding angle distribution (see also Appendix A). The relation between extension and supercoiling degree can also be obtained by fixing the external force and changing the value of the applied torque. To calculate the ground-state eigenvalue and eigenfunctions of an asymmetric matrix turns out to be complicated and time-consuming. Fortunately, as we have calculated in Appendix B, each eigenfunction of Eq. (23) shares the same quantity m; the matrix for $m = 0$ is still Hermitian and can be diagonalized by unitary matrices. The ground-state eigenvalue for $m = 0$ is lower in several order than those for $m \neq 0$ in the whole relevant region of external torque Γ from $-5.0k_BT$ to $5.0k_BT$. Thus, actually we only need to consider the case of $m = 0$ and in this case we still have $\chi_0(\mathbf{t},\varphi) = \Phi_0^*(\mathbf{t},\varphi)$. The whole procedure we have performed in Sec. III can safely be repeated in this section, and the relationships between force and extension and between torque and linking number can be consequently calculated.

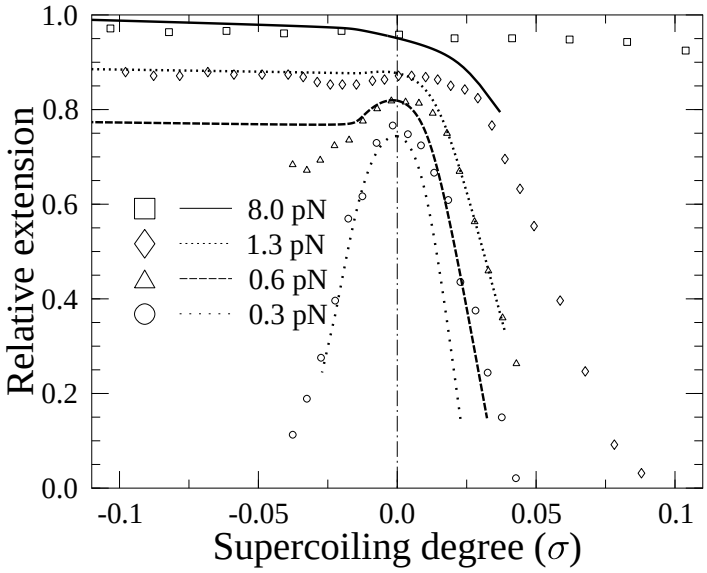

FIG. 5. Extension vs supercoiling relations at fixed pulling forces for torsionally constrained DNA. The parameters for the curves are the same as Fig. 2 and experimental data is from Fig. 3 of [13] (symbols).

To make the calculation further easier and also to make sure that the above-mentioned calculation is indeed correct, we introduce here an approximate method which reduces the computational complexity considerably. It turns out that the calculated results using this method are in considerable agreement with the above-mentioned precise method. In the experiment of Ref. [13], the applied external forces change in the region of 0.3 pN to 10 pN. In this region, as demonstrated in Figs. 3 and 4, both the tangential ($\mathbf{t}$) and the folding angle (φ) fluctuations of dsDNA molecules are small. Taking into account this fact, then in Eq. (14), the energy term $\kappa^*(d\mathbf{t}/ds)^2$ can be approximately calculated to be $\kappa^*((dt_x/ds)^2 + (dt_y/ds)^2)$, and $f\mathbf{t}\cdot\mathbf{z}_0\cos\varphi \simeq f\cos\varphi - f\langle\cos\varphi\rangle(t_x^2 + t_y^2)/2$. Thus, Eq. (14) is decomposed into two "independent" parts. The first part is only related to φ. At each value of f and Γ, we can calculate the average quantities $\langle\cos\varphi\rangle$ and $\langle\sin\varphi\rangle$ based on this energy using the method of path integral. The second part is quadratic in t_x and t_y, therefore the average values of $\mathbf{t}\cdot\mathbf{z}_0$ and Wr (Eq. (11)) can be obtained analytically. Using this decomposition and preaveraging technique, the average extension and average supercoiling degree can both be

calculated at each value of external force and torque, and the relation between extension and linking number at fixed forces can be then obtained.

The theoretical relationship between extension and supercoiling degree is shown in Fig. 5 and compared with the experiment of Strick *et al.* [13]. In obtaining these curves, the values of the parameters are the same as those used in Fig. 2 and no adjustment has been done to fit the experimental data. We find that in the case of negatively supercoiled DNA, the theoretical and experimental results are in quantitative agreement, indicating that the present model is capable of explaining the elasticity of negatively supercoiled DNA; in the case of positively supercoiled DNA, the agreement between theory and experiment is not so good, especially when the external force is relatively large. In our present work, we have not considered the possible deformations of the nucleotide basepairs. While this assumption might be reasonable in the negatively supercoiled case, it may fail for positively supercoiled DNA chain, especially at large stretching forces. The work done by Allemand *et al.* [15] suggested that positive supercoiled and highly extended DNA molecule can take on Pauling-like configurations with exposed bases. To better understand the elastic property of positively supercoiled DNA, it is certainly necessary for us to take into account the deformations of basepairs.

For negatively supercoiled DNA molecule, both theory and experiment reveal the following elastic aspects: (a) When external force is small, DNA molecule can shake off its torsional stress by writhing its central axis, which can lead to an increase in the negative writhing number and hence restore the local folding manner of DNA strands to that of B-form DNA: (b) However, writhing of the central axis causes shortening of DNA end-to-end extension, which becomes more and more unfavorable as the external force is increased. Therefore, at large forces, the torsional stress caused by negative torque (supercoiling degree) begins to unwind the B-form double-helix and triggers the transition of DNA internal structure, where a continuously increasing portion of DNA takes on some certain new configuration as supercoiling increases, while its total extension keeps almost invariant. Our Monte Carlo simulations have also confirmed the above insight [44].

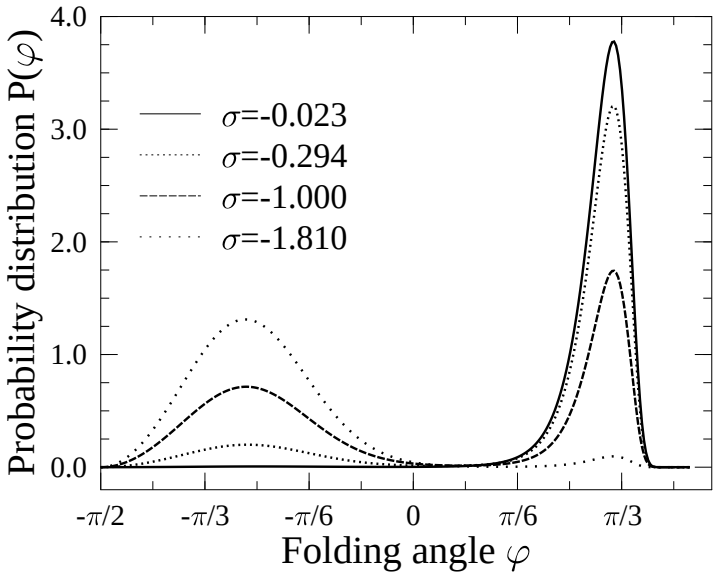

FIG. 6. Folding angle distributions for negatively supercoiled DNA molecule pulled with a force of 1.3 pN.

What is the new configuration? According to the opinion of Ref. [13], such new configuration corresponds to denatured DNA segments, i.e., negative torque leads to breakage of hydrogen bonds between the complementary DNA bases and consequently to strand-separation. They have also done an elegant experiment in which short single-stranded homologous DNA segments are inserted into the experimental buffer [14]. They found that, in confirmative with their insight, these homologous DNA probes indeed bind onto negatively supercoiled dsDNA molecules. Recently, Léger *et al.* [16] have also done experiment on single dsDNA molecules. To explain qualitatively their experimental result, they found that left-handed Z-form DNA should be considered as a possible configuration for negatively

supercoiled dsDNA chain, while the molecules need not be denatured. As seen in Fig. 5, although the present model has not taken into account the possibility of strand-separation, it can quantitatively explain the behavior of negatively supercoiled DNA. Therefore, it may be helpful for us to investigate the possibility of formation of left-handed configurations based on our present model. This effort is done in the next subsection, where the energetics of such configurations will also be discussed.

B. Possible left-handed DNA configurations

We have mentioned in Sec. II A that left-handed configurations correspond to $\varphi < 0$ in our present model (see also Fig. 1). Based on the present model, then information about the new configuration mentioned in Sec. IV A can be revealed by the folding angle distributions $P(\varphi)$, as have been discussed in Sec. III. In the present case, $P(\varphi)$ is calculated as follows:

$$P(\varphi) = \int \chi_0(\mathbf{t}, \varphi)\Phi_0(\mathbf{t}, \varphi)d\mathbf{t}, \tag{27}$$

where, as mentioned in Sec. IV A, $\Phi_0(\mathbf{t}, \varphi)$ and $\chi_0(\mathbf{t}, \varphi)$ are, respectively, the ground-state right- and left-eigenfunction of Eq. (23); and actually, $\chi_0(\mathbf{t}, \varphi) = \Phi_0^*(\mathbf{t}, \varphi)$.

The calculated folding angle distribution [45] is shown in Fig. 6, which is radically different with that of torsionally relaxed dsDNA molecules shown in Fig. 3. It has the following aspects: When the torsional stress is small (with the supercoiling degree $|\sigma| < 0.025$), the distribution has only one narrow and steep peak at $\varphi \simeq +57.0°$, indicating that DNA is completely in B-form. With the increase of torsional stress, however, another peak appears at $\varphi \simeq -48.6°$ and the total probability for the folding angle to be negatively-valued increases gradually with supercoiling. Since negative folding angles correspond to left-handed configurations, the present model suggests that, with the increasing of supercoiling, left-handed DNA conformation is nucleated and it then elongates along the DNA chain as B-DNA disappears gradually. The whole chain becomes completely left-handed at $\sigma \simeq -1.85$.

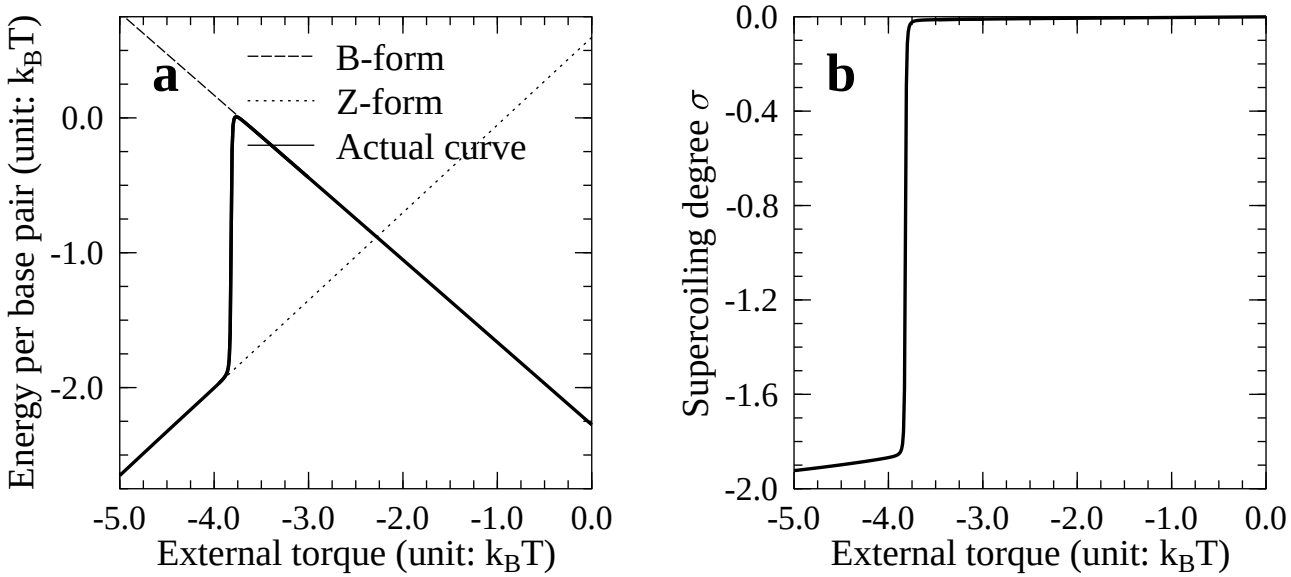

FIG. 7. (A), The sum of the average base-stacking and torsional energy per basepair at force 1.3 pN. For highly extended DNA only these two interactions are sensitive with torque. (B), The relation between DNA supercoiling degree and external torque at force 1.3 pN.

It is worth to be noticed that, (a) as the supercoiling degree changes, the positions of the two peaks of the folding angle distribution remain almost fixed and, (b) between these two peaks, there exists an extended region of folding angle from 0 to $\pi/6$ which always has only extremely small probability of occurrence. Thus, a negatively supercoiled DNA can have two possible stable configurations, a right-handed B-form and a left-handed configuration with an

average folding angle $\simeq -48.6°$. A transition between these two structures for a DNA segment will generally lead to an abrupt and finite variation in the folding angle.

To obtain the energetics of such transitions, we have calculated how the sum of the base-stacking energy and torsional energy, $(\kappa/R^2)\sin^4\varphi + \rho(\varphi) - (\Gamma/R)\sin\varphi$, changes with external torque [45]. Figure 7a shows the numerical result, and Fig. 7b demonstrates the relation between supercoiling degree and external torque. (In both figures the external force is fixed at 1.3 pN.) From these figures we can infer that, (a) for negative torque less than the critical value $\Gamma_c \simeq -3.8$ k_BT, DNA can only stay in B-form state; (b) near this critical torque, DNA can either be right- or be left-handed and, as negative supercoiling increases (see Fig. 7b) more and more DNA segments will stay in the left-handed form, which is much lower in energy ($\simeq -2.0$ k_BT per basepair) but stable only when torque reaches Γ_c; (c) for negative torque greater than Γ_c DNA is completely left-handed.

Nevertheless, we should emphasize that the above calculations are all based on our present model which has assumed that nucleotide basepairs do not break. Figure 5 indicates that for negatively supercoiled DNA chains, the extension vs supercoiling degree relation can be quantitatively explained by the present model; and Fig. 6 reveals the reason of the quantitative agreement is that the present model allows the possibility of occurrence of left-handed DNA configurations. At the present time, to say that negatively supercoiled DNA will prefer left-handed configurations rather than denaturation and strand-separation is premature. To clarify this question, the present model should be improved to consider the deformations of DNA basepairs. In the experimental side, it might also be helpful to measure precisely the critical torque at which the elastic behavior of negatively supercoiled DNA changes abruptly and compare the measured results with the value calculated in the present work. (In the earlier experiment of Allemand *et al.* [15], the critical torque is estimated to be $\sim -2k_BT$ by assuming that the torsional rigidity of dsDNA to be 75 nm and that torsional stress builds up linearly along the DNA chain. This value, however, maybe not precise enough since the torsional rigidity of dsDNA molecule is not a precisely determined quantity and the values giving by different groups are scattered widely.[5]

The structural parameters of the left-handed configuration suggested by Figs. 6 and 7 are listed in table I [45] and compared with those of Z-form DNA [2]. The strong similarity in these parameters suggests that the torque-induced left-handed configurations, if they really exist, belong to Z-form DNA [2,16,45].

TABLE I. For the torque-induced left-handed DNA configuration, the average rise per basepair (d), the pitch per turn of helix, and the number of basepairs per turn of helix (num) are calculated and listed under different external forces and torques. The last row contains the corresponding values for Z-form DNA.

force (pN)	torque (k_BT)	d (Å)	pitch (Å)	num
1.3	-5.0	3.59	41.20	11.48
1.0	-5.0	3.57	40.93	11.44
1.3	-4.0	3.83	46.76	12.19
1.0	-4.0	3.82	46.38	12.15
Z-form:		3.8	45.6	12

[5]Another possibility may be that we have over-estimated the value of the critical torque. It maybe possible that the transition from right- to left-handed configurations is initiated in the weaker AT-rich regions, whose value of ϵ should be less than the average value taken by the present paper.

V. CONCLUSION

In this article, we have presented an elastic model for double-stranded biopolymers such as DNA molecules. The key progress is that the bending deformations of the backbones of DNA molecules and the base-stacking interactions existing between adjacent DNA basepairs are quantitatively considered in this model, with the introduction of a new structural parameter, the folding angle φ. This model has also qualitatively taken into account the effects of the steric effects of DNA basepairs and electrostatic interactions along DNA chain. In calculation technique, the model is investigated using path integral method; and Green equations similar in form to the Schrödinger equation in quantum mechanics are derived and their ground-state eigenvalues and eigenfunctions obtained by precise numerical calculations. The force-extension relationship in torsionally relaxed and the extension-linking number relationship in torsionally constrained DNA chains are studied and compared with experimental results. This work demonstrated that DNA molecule's entropic elasticity and highly extensibility, as well as the elastic property of negatively supercoiled DNA can all be quantitatively explained by the present theory. The comprehensive agreement between theory and experiments indicated that the short-ranged base-stacking interactions are very important in determining the elastic response of double-stranded DNA molecules. The present work showed that highly extended and negatively supercoiled DNA molecules can be left-handed, probably in the Z-form configuration. A possible way to check the validity of this opinion is to measure the critical external torque at which the transition between B-form DNA and the new configuration takes place.

The present work regarded DNA basepairs as rigid objects and did not consider their possible deformations and the possibility of strand-separation. The comprehensive agreement between theory and experiments indicates that this approach is well justified in many cases. However, as already mentioned in Sec. II A, under some extreme conditions, this assumption may not be appropriate. For example, recent experimental work of Allemand *et al.* [15] showed that positively supercoiled DNA under high applied force can take on Pauling-like configurations with exposed bases. In this case the basepairing of DNA is severely distorted, and because the present model has not taken into account the possible deformations of the basepairs, the theoretical results on positively supercoiled DNA molecules were not in quantitative agreement with experiment (see Fig. 5). Furthermore, although the present work showed that left-handed DNA configurations can be stabilized by negative torques, much theoretical work is still needed to calculate the denaturation free energy and be compared with the free energy of left-handed DNA configurations.

VI. ACKNOWLEDGEMENT

It gives us great pleasure to acknowledge the helps and valuable suggestions of our colleagues, especially Lou Ji-Zhong, Liu Lian-Shou, Yan Jie, Liu Quan-Hui, Zhou Xin, Zhou Jian-Jun, and Zhang Yong. The numerical calculations are performed partly at ITP-Net and partly at the State Key Lab. of Scientific and Engineering Computing.

APPENDIX A: PATH INTEGRAL METHOD IN POLYMER PHYSICS

In this appendix we review some basic ideas on the application of path integral method to the study of polymeric systems [39]. Consider a polymeric string, and suppose its total "arclength" is L, and along each arclength point s one can define a n-dimensional "vector" $\mathbf{r}(s)$ to describe the polymer's local state at this point.[6] We further assume that the energy density (per unit arclength) of the polymer can be written as the following general form:

$$\rho_e(\mathbf{r}, s) = \frac{m}{2}(\frac{d\mathbf{r}}{ds})^2 + \mathbf{A}(\mathbf{r}) \cdot \frac{d\mathbf{r}}{ds} + V(\mathbf{r}), \tag{A1}$$

where $V(\mathbf{r})$ is a scalar field and $\mathbf{A}(\mathbf{r})$ is a vectorial field. The total partition function of the system is expressed by the following integration:

$$\Xi(L) = \int\int d\mathbf{r}_f \phi_f(\mathbf{r}_f) G(\mathbf{r}_f, L; \mathbf{r}_i, 0) \phi_i(\mathbf{r}_i) d\mathbf{r}_i, \tag{A2}$$

[6]For example, in the case of a flexible Gaussian chain, $\mathbf{r}$ is a three-dimensional position vector; in the case of a semiflexible chain such as the wormlike chain [18,41], $\mathbf{r}$ is the unit tangent vector of the polymer and is two-dimensional.

where $\phi_i(\mathbf{r})$ and $\phi_f(\mathbf{r})$ are, respectively, the probability distributions of the vector $\mathbf{r}$ at the initial ($s = 0$) and final ($s = L$) arclength point; $G(\mathbf{r}, s; \mathbf{r}', s')$ is called the Green function, it is defined in the following way:

$$G(\mathbf{r}, s; \mathbf{r}', s') = \int_{\mathbf{r}'}^{\mathbf{r}} \mathcal{D}[\mathbf{r}''(s)] \exp[-\beta \int_{s'}^{s} ds'' \rho_e(\mathbf{r}'', s'')], \tag{A3}$$

where integration is carried over all possible configurations of $\mathbf{r}''$, and $\beta = 1/k_B T$ is the Boltzmann coefficient. It can be verified that the Green function defined above satisfies the following relation [39]:

$$G(\mathbf{r}, s; \mathbf{r}', s') = \int d\mathbf{r}'' G(\mathbf{r}, s; \mathbf{r}'', s'') G(\mathbf{r}'', s''; \mathbf{r}', s'), \quad (s' < s'' < s). \tag{A4}$$

The total free energy of the system is then expressed as

$$\mathcal{F} = -k_B T \ln \Xi. \tag{A5}$$

To calculate the total partition function Ξ, we define an auxiliary function $\Psi(\mathbf{r}, s)$ and call it the wave function because of its similarity with the true wave function of quantum systems. Suppose the value of Ψ at arclength point s is related to its value at s' through the following formula such that[7]

$$\Psi(\mathbf{r}, s) = \int d\mathbf{r}' G(\mathbf{r}, s; \mathbf{r}', s') \Psi(\mathbf{r}', s'), \quad (s > s') \tag{A6}$$

then, we can derive from Eqs. (A1), (A3), and (A6) that [39]:

$$\frac{\partial \Psi(\mathbf{r}, s)}{\partial s} = \left[\frac{\nabla_{\mathbf{r}}^2}{2m\beta} - \beta V(\mathbf{r}) + \frac{\mathbf{A}(\mathbf{r}) \cdot \nabla_{\mathbf{r}}}{m} + \frac{\nabla_{\mathbf{r}} \cdot \mathbf{A}(\mathbf{r})}{2m} + \frac{\beta \mathbf{A}^2(\mathbf{r})}{2m} \right] \Psi(\mathbf{r}, s) = \hat{H} \Psi(\mathbf{r}, s). \tag{A7}$$

Equation (A7) is called the Green equation, it is very similar with the Schrödinger equation of quantum mechanics [40]. However, there is an important difference. In the case of $\mathbf{A}(\mathbf{r}) \neq 0$, the operator $\hat{H}$ in Eq. (A7) is not Hermitian. Therefore, in this case the matrix form of the operator $\hat{H}$ may not be diagonalized by unitary matrix.

Denote the eigenvalues and the right-eigenfunctions of Eq. (A7) as $-g_i$ and $|i\rangle = \Phi_i(\mathbf{r})$ ($i = 0, 1, \cdots$), respectively. Then it is easy to know, from the approach of quantum mechanics, that

$$\Psi(s) = \sum_i e^{-g_i(s-s')} |i(s)\rangle \langle i(s')|\Psi(s')\rangle, \tag{A8}$$

where $\langle i| = \chi_i(\mathbf{r})$ ($i = 0, 1, \cdots$) denote the left-eigenfunctions of Eq. (A7), which satisfy the following relation:

$$\langle i|i'\rangle = \int d\mathbf{r} \chi_i(\mathbf{r}) \Phi_{i'}(\mathbf{r}) = \delta_i^{i'}.$$

In the case where $\hat{H}$ is Hermitian (i.e., $\mathbf{A}(\mathbf{r}) = 0$), then we can conclude that

$$\chi_i(\mathbf{r}) = \Phi_i^*(\mathbf{r}).$$

From Eqs. (A2), (A6), (A7), and (A8) we know that

$$\begin{aligned} \Xi(L) &= \int d\mathbf{r} \int d\mathbf{r}' G(\mathbf{r}, L; \mathbf{r}', s') \phi_f(\mathbf{r}) \phi_i(\mathbf{r}') = \sum_i \langle \phi_f|i\rangle \langle i|\phi_i\rangle e^{-g_i L} \\ &= e^{-g_0 L} \langle \phi_f|0\rangle \langle 0|\phi_i\rangle \qquad (\text{for } \; L \gg 1/(g_1 - g_0)). \end{aligned} \tag{A9}$$

Consequently, for long polymer chains the total free energy density is just expressed as

$$\mathcal{F}/L = k_B T g_0, \tag{A10}$$

---

[7] In fact, the choice of the wave function $\Psi(\mathbf{r}, s)$ is not limited. Any function determined by an integration of the form of Eq. (A6) can be viewed as a wave function.

and any quantity of interest can then be calculated by differentiation of $\mathcal{F}$. For example, the average extension of a polymer under external force field f can be calculated as $\langle Z\rangle = \partial\mathcal{F}/\partial f = Lk_BT\partial g_0/\partial f$.

We continue to discuss another very important quantity, the distribution probability of $\mathbf{r}$ at arclength s, $P(\mathbf{r},s)$. This probability is calculated from the following expression:

$$P(\mathbf{r},s) = \frac{\int d\mathbf{r}_f \int d\mathbf{r}_i \phi_f(\mathbf{r}_f) G(\mathbf{r}_f, L; \mathbf{r}, s) G(\mathbf{r}, s; \mathbf{r}_i, 0)\phi_i(\mathbf{r}_i)}{\int d\mathbf{r}_f \int d\mathbf{r}_i \phi_f(\mathbf{r}_f) G(\mathbf{r}_f, L; \mathbf{r}_i, 0)\phi_i(\mathbf{r}_i)}. \tag{A11}$$

Based on Eqs. (A6) and (A8) we can rewrite Eq. (A11) in the following form:

$$\begin{aligned} P(\mathbf{r},s) &= \frac{\int d\mathbf{r}_f \int d\mathbf{r}_i \int d\mathbf{r}' \phi_f(\mathbf{r}_f) G(\mathbf{r}_f, L; \mathbf{r}', s)\delta(\mathbf{r}'-\mathbf{r}) G(\mathbf{r}, s; \mathbf{r}_i, 0)\phi_i(\mathbf{r}_i)}{\int d\mathbf{r}_f \int d\mathbf{r}_i \phi_f(\mathbf{r}_f) G(\mathbf{r}_f, L; \mathbf{r}_i, 0)\phi_i(\mathbf{r}_i)} \\ &= \frac{\sum\limits_m \sum\limits_n \langle\phi_f|m\rangle\langle n|\phi_i\rangle \chi_m(\mathbf{r})\Phi_n(\mathbf{r}) \exp[-g_m(L-s) - g_n s]}{\sum\limits_m \langle\phi_f|m\rangle\langle m|\phi_i\rangle \exp(-g_m L)} \end{aligned} \tag{A12}$$

For the most important case of $0 \ll s \ll L$, Eq. (A12) then gives that the probability distribution of $\mathbf{r}$ is independent of arclength s, i.e.,

$$P(\mathbf{r},s) = \chi_0(\mathbf{r})\Phi_0(\mathbf{r}) \quad (\text{for } \ 0 \ll s \ll L). \tag{A13}$$

With the help of Eq. (A13), the average value of a quantity which is a function of $\mathbf{r}$ can be obtained. For example,

$$\langle Q(s)\rangle = \int d\mathbf{r} Q(\mathbf{r}) P(\mathbf{r},s) = \int d\mathbf{r} \chi_0(\mathbf{r}) Q(\mathbf{r}) \Phi_0(\mathbf{r}) = \langle 0|Q|0\rangle, \tag{A14}$$

and

$$\langle \int_0^L Q(\mathbf{r}(s)) ds\rangle = \int_0^L \langle Q(s)\rangle ds = L\langle 0|Q|0\rangle \quad (\text{for } \ L \gg 1/(g_1 - g_0)). \tag{A15}$$

Finally, we list the formula for calculating $\langle \mathbf{B}(\mathbf{r}) \cdot d\mathbf{r}/ds\rangle$, here $\mathbf{B}(\mathbf{r})$ is a given vectorial field. The formula reads:

$$\langle \mathbf{B}(\mathbf{r}) \cdot \frac{d\mathbf{r}}{ds}\rangle = \frac{1}{2}\langle 0| \left[\mathbf{r}\cdot(\hat{H}\mathbf{B}) - \mathbf{B}\cdot(\hat{H}\mathbf{r})\right] |0\rangle \quad (\text{for } \ L \gg 1/(g_1 - g_0)). \tag{A16}$$

APPENDIX B: MATRIX FORMALISM OF THE GREEN EQUATION EQ. (23)

In Eq. (23) (and also Eq. (15)) the variables $\mathbf{t}$ and φ are coupled together. Denote the operator in the square brackets of Eq. (23) as $\hat{H}$. We express this operator in matrix form. To this end we choose the base functions of this system to be the combinations of spherical harmonics $Y_{lm}(\theta,\phi)$ and $f_n(\tilde{\varphi})$ (see Eq. (20)).

For $m = 0$, the base functions are expressed to be

$$|i\rangle = |l\cdot N_\varphi + n\rangle = |l; n\rangle = Y_{l0}(\theta,\phi) f_n(\tilde{\varphi}); \tag{B1}$$

and for $m = 1, 2, \cdots$, the base functions are expressed to be

$$|i\rangle = |2(l-m)\cdot N_\varphi + 2(n-1) + k\rangle = |l; n; k\rangle = Y_{lm}^{(k)}(\theta,\phi) f_n(\tilde{\varphi}). \tag{B2}$$

In the above two equations, $n = 1, 2, \cdots, N_\varphi$ with N_φ set to be 60 in our present calculations; $l = 0, 1, \cdots, N_l - 1$ for the case of $m = 0$ (with N_l set to 30), or $l = m, m+1, \cdots, m + N_l - 1$ for the case of $m \neq 0$ (with N_l set to 15); $k = 1, 2$; and

$$\begin{aligned} Y_{l0}(\theta,\phi) &= \sqrt{\frac{2l+1}{4\pi}} P_l(\cos\theta), \\ Y_{lm}^{(1)}(\theta,\phi) &= (-1)^m \sqrt{\frac{2l+1}{2\pi}\frac{(l-m)!}{(l+m)!}} P_l^m(\cos\theta)\cos(m\phi), \\ Y_{lm}^{(2)}(\theta,\phi) &= (-1)^m \sqrt{\frac{2l+1}{2\pi}\frac{(l-m)!}{(l+m)!}} P_l^m(\cos\theta)\sin(m\phi). \end{aligned}$$

With the above definitions, we then obtain that, for $m = 0$:

$$\begin{aligned}
\langle i_p|(-\hat{H})|i\rangle &= \langle l_p; n_p|(-\hat{H})|l; n\rangle \\
&= \delta_l^{l_p}\delta_n^{n_p}\left[\frac{l(l+1)}{4\ell_p^*} + \frac{n^2\pi^2}{4\ell_p a^2}\right] \\
&- \frac{f}{k_BT}\left[\delta_{l_p}^{l+1}a_{l,0} + \delta_{l_p}^{l-1}a_{l-1,0}\right]\langle n_p|\sin\tilde{\varphi}|n\rangle \\
&+ \delta_{l_p}^{l}\langle n_p|\left[\frac{\rho(\tilde{\varphi})}{k_BT} + \frac{\ell_p}{R^2}\cos^4\tilde{\varphi}\right]|n\rangle \\
&+ \delta_{l_p}^{l}\frac{\Gamma}{Rk_BT}\langle n_p|\cos\tilde{\varphi}|n\rangle \\
&- \delta_{n_p}^{n}\frac{\Gamma^2}{16\ell_p^*(k_BT)^2}\left[\delta_{l_p}^{l}(1 - a_{l,0}^2 - a_{l-1,0}^2) - \delta_{l_p}^{l+2}a_{l,0}a_{l+1,0} - \delta_{l_p}^{l-2}a_{l-1,0}a_{l-2,0}\right];
\end{aligned} \tag{B3}$$

and for $m \neq 0$:

$$\begin{aligned}
\langle i_p|(-\hat{H})|i\rangle &= \langle l_p; n_p; k_p|(-\hat{H})|l; n; k\rangle \\
&= \delta_{l_p}^{l}\delta_{n_p}^{n}\delta_{k_p}^{k}\left[\frac{l(l+1)}{4\ell_p^*} + \frac{n^2\pi^2}{4\ell_p a^2}\right] \\
&- \frac{f}{k_BT}\delta_{k_p}^{k}\left[\delta_{l_p}^{l+1}a_{l,m} + \delta_{l_p}^{l-1}a_{l-1,m}\right]\langle n_p|\sin\tilde{\varphi}|n\rangle \\
&+ \delta_{l_p}^{l}\delta_{k_p}^{k}\langle n_p|\left[\frac{\rho(\tilde{\varphi})}{k_BT} + \frac{\ell_p}{R^2}\cos^4\tilde{\varphi}\right]|n\rangle \\
&+ \delta_{l_p}^{l}\delta_{k_p}^{k}\frac{\Gamma}{Rk_BT}\langle n_p|\cos\tilde{\varphi}|n\rangle + \delta_{l_p}^{l}\delta_{n_p}^{n}\frac{\Gamma}{4\ell_p^*k_BT}(k - k_p)m \\
&- \delta_{n_p}^{n}\delta_{k_p}^{k}\frac{\Gamma^2}{16\ell_p^*(k_BT)^2}\left[\delta_{l_p}^{l}(1 - a_{l,m}^2 - a_{l-1,m}^2) - \delta_{l_p}^{l+2}a_{l,m}a_{l+1,m} - \delta_{l_p}^{l-2}a_{l-1,m}a_{l-2,m}\right].
\end{aligned} \tag{B4}$$

In Eqs. (B3) and (B4), the following notations are used:

$$\begin{aligned}
a_{l,m} &= \sqrt{\frac{(l+1)^2 - m^2}{(2l+1)(2l+3)}}, \\
\langle n_p|y(\tilde{\varphi})|n\rangle &= \frac{2}{a}\int_0^a \sin(\frac{n_p\pi\tilde{\varphi}}{a})y(\tilde{\varphi})\sin(\frac{n\pi\tilde{\varphi}}{a}),
\end{aligned}$$

where $y(\tilde{\varphi})$ is any function of $\tilde{\varphi}$.

The ground-state eigenvalues of the matrices Eq. (B3) and Eq. (B4) have been calculated at force 1.3 pN in the whole relevant region of Γ from $-5.0k_BT$ to $+5.0k_BT$. We have found that the ground-state eigenvalues for the case of $m = 0$ are of the order of -10 nm^{-1}; while those for the case of $m \neq 0$ are of the order of 10^6 nm^{-1} (data not shown). Thus, we can conclude with confidence that the "low energy" eigenstates of the system all have the same $m = 0$. This can greatly reduce the calculation tasks.

As a final point, here we demonstrate how to calculate the average values of the quantities of our interest. Suppose $y(\mathbf{t}, \tilde{\varphi})$ is a quantity whose average value we are interested in. Denote $\mathcal{U}$ as the unitary matrix which can diagonalize the matrix Eq. (B3). (Because the matrix Eq. (B3) is real symmetric, $\mathcal{U}$ is actually a real orthogonal matrix.) Then its column vector $\mathbf{u}(i) = \sum_j \mathcal{U}(j,i)|j\rangle$ $(i = 1, 2, \cdots)$ corresponds to the i-th eigenvector of Eq. (B3). Consequently, we can calculate based on Eq. (A14) that

$$\langle y(\mathbf{t}, \tilde{\varphi})\rangle = \sum_{i,i_p}\mathcal{U}(i_p, 1)\mathcal{U}(i, 1)\langle i_p|y(\mathbf{t}, \tilde{\varphi})|i\rangle. \tag{B5}$$

* Electronic address: zhouhj@itp.ac.cn.

[1] W. Saenger, *Principles of Nucleic Acid Structure* (Springer-Verlag, New York, 1984).
[2] J. D. Watson *et al.*, *Molecular Biology of the Gene* (Benjamin/Cummings Pub., California, 1987), 4th edition.
[3] T. Nishinaka, Y. Ito, S. Yokoyama, and T. Shibata, Proc. Natl. Acad. Sci. U.S.A **94**, 6623 (1997).
[4] T. Nishinaka, A. Shinohara, Y. Ito, S. Yokoyama, and T. Shibata, *ibid.* **95**, 11071 (1998).
[5] J. F. Léger, J. Robert, L. Bourdieu, D. chatenay, and J. F. Marko, *ibid.* **95**, 12 295 (1998).
[6] L. Stewart, M. R. Redinbo, X. Qiu, W. G. J. Hol, and J. J. Champoux, Science **279**, 1534 (1998).
[7] V. V. Rybenkov, C. Ullsperger, A. V. Vologodskii, N. R. Cozzarelli, Science **277**, 690 (1997).
[8] J. Yan, M. O. Magnasco, and J. F. Marko, Nature (London) **401**, 932 (1999).
[9] S. B. Smith, L. Finzi, and C. Bustamante, Science **258**, 1122 (1992).
[10] D. Bensimon, A. J. Simon, V. Croquette, and A. Bensimon, Phys. Rev. Lett. **74**, 4754 (1995).
[11] P. Cluzel, A. Lebrun, C. Heller, R. Lavery, J.-L. Viovy, D. Chatenay, and F. Caron, Science **271**, 792 (1996).
[12] S. B. Smith, Y. Cui, and C. Bustamante, *ibid.* **271**, 795 (1996).
[13] T. R. Strick, J.-F. Alleman, D. Bensimon, A. Bensimon, and V. Croquette, *ibid.* **271**, 1835 (1996).
[14] T. R. Strick, V. Croquette, and D. Bensimon, Proc. Natl. Acad. Sci. U.S.A **95** 10 579 (1998).
[15] J. F. Allemand, D. Bensimon, R. Lavery, and V. Croquette, *ibid.* **95**, 14 152 (1998).
[16] J. F. Léger, G. Romano, A. Sarkar, J. Robert, L. Bourdieu, D. chatenay, and J. F. Marko, Phys. Rev. Lett. **83**, 1066 (1999).
[17] C. Bustamante, J. F. Marko, E. D. Siggia, and S. Smith, Science **265**, 1599 (1994).
[18] J. F. Marko and E. D. Siggia, Macromolecules **28**, 8759 (1995).
[19] M.-H. Hao and W. K. Olson, Biopolymers **28**, 873 (1989); Macromolecules **22**, 3292 (1989).
[20] B. Fain, J. Rudnick, and S. Östlund, Phys. Rev. E **55**, 7364 (1996).
[21] J. F. Marko, Europhys. Lett. **38**, 183 (1997); Phys. Rev. E **57**, 2134 (1998).
[22] J. D. Moroz and P. Nelson, Proc. Natl. Acad. Sci. U.S.A **94**, 14 418 (1997).
[23] A. V. Vologodskii and J. F. Marko, Biophys. J. **73**, 123 (1997).
[24] B.-Y. Ha and D. Thirumalai, J. Chem. Phys. **106**, 4243 (1997).
[25] P. Cizeau and J.-L. Viovy, Biopolymers **42**, 383 (1997).
[26] C. Bouchiat and M. Mézard, Phys. Rev. Lett. **80**, 1556 (1998); cond-mat/9904018 (1999).
[27] P. Nelson, Phys. Rev. Lett. **80**, 5810 (1998).
[28] Zhou Haijun and Ou-Yang Zhong-Can, Phys. Rev. E **58**, 4816 (1998); J. Chem. Phys. **110**, 1247 (1999).
[29] Zhou Haijun, Zhang Yang, and Ou-Yang Zhong-Can, Phys. Rev. Lett. **82**, 4560 (1999).
[30] R. Everaers, R. Bundschuh, and K. Kremer, Europhys. Lett. **29**, 263 (1995).
[31] T. B. Liverpool, R. Golestanian, and K. Kremer, Phys. Rev. Lett. **80**, 405 (1998).
[32] L. Stryer, *Biochemistry* (Freeman and Company, New York. 1995), 4th edition.
[33] T. T. Perkins, D. E. Smith, S. Chu, Science **276**, 2016 (1997) and references cited therein.
[34] J. H. White, Am. J. Math. **91**, 693 (1969).
[35] F. B. Fuller, Proc. Natl. Acad. Sci. U.S.A. **68**, 815 (1971).
[36] F. H. C. Crick, *ibid.* **73**, 2639 (1976).
[37] J. H. White and W. R. Bauer, *ibid.* **85**, 772 (1988).
[38] F. B. Fuller, *ibid.* **75**, 3557 (1978).
[39] Zhou Haijun, unpublished notes; see also: M. Doi and S. F. Edwards, *The Theory of Polymer Dynamics* (Clarendon Press, Oxford, 1986); H. Kleinert, *Path Integrals in Quantum Mechanics, Statistics, and Polymer Physics* (World Scientific, Singapore, 1990).
[40] J. Y. Zeng, *Quantum Mechanics* (Academic Press, Beijing, 1999), 2nd edition (in Chinese), Vol. I.
[41] K. Kroy and E. Frey, Phys. Rev. Lett. **77**, 306 (1996).
[42] G. V. Shivashankar, M. Feingold, O. Krichevsky, and A. Libchaber, Proc. Natl. Acad. Sci. U.S.A. **96**, 7912 (1999).
[43] M. Hegner, S. B. Smith, and C. Bustamante, *ibid.* **96**, 10 109 (1999).
[44] Zhang Yang, Zhou Haijun, and Ou-Yang Zhong-Can, Biophys. J. **78**, 1979 (2000).
[45] Zhou Haijun and Ou-Yang Zhong-Can, Mod. Phys. Lett. B, (2000, in press); see also cond-mat/9908129.